Journal of Power Sources 262 (2014) 263–269

Contents lists available at ScienceDirect

Journal of Power Sources

journal homepage: www.elsevier.com/locate/jpowsour

Multivariate investigation of parameters in the development and improvement of NiFe cells

Jorge Omar Gil Posada*, Peter J. Hall

Chemical and Biological Engineering, University of Sheffield, Sir Robert Hadfield Building, Mapping Street, Sheffield S1 1XJ, England, UK

HIGHLIGHTS

- We investigate bismuth sulphide as an additive for the production of NiFe cells.
- We conduct an experimental design in order to improve NiFe cell formulations.
- The performance of a NiFe Cell depends on the initial cycles of charge/discharge.
- The reactivity of an iron electrode depends on its degree of passivation.

GRAPHICAL ABSTRACT

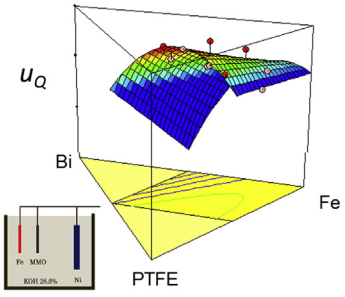

ARTICLE INFO

Article history:
Received 31 January 2014
Received in revised form
25 March 2014
Accepted 29 March 2014
Available online 4 April 2014

Keywords:
NiFe cell
Iron electrode
Coulombic efficiency
Battery testing

ABSTRACT

In this article, we use a surface response approach to investigate the effect of bismuth sulphide as well as the compositions of PTFE in the overall columbic efficiency of a NiFe cell battery. Our results demonstrate that while bismuth sulphide favours the process of charge/discharge of a NiFe cell, the use of metallic bismuth only marginally influences coulombic efficiency. In addition we had found that the presence of the soluble bisulfide anion is not sufficient to increase coulombic efficiency in NiFe cells.

1. Introduction

Successfully commercialised in the early 1900's [1], nickel/Iron (NiFe) batteries are rechargeable energy storage devices that fell out of favour with the advent of cheaper lead-acid cells. There has been a resurgence of interest in NiFe cells arising from their compatibility with photovoltaics (PV) as they are seen to be more cost-effective and environmentally friendly than their lead-acid counterparts [2].

There are many advantages favouring the use of NiFe cells such as robustness, longevity, environmental friendliness and the relatively low cost of bulk raw materials. However, NiFe cells are limited by their relatively low energy and power densities. A further drawback is the relatively low efficiency of the charge–discharge cycle, with energy efficiencies of 50–60% being widely quoted [2,3].

2. Theory

The primary process that takes place during the charging of an iron electrode is the reduction of iron (II) to metallic iron as

* Corresponding author. Tel.: +44 (0)1142228257; fax: +44 (0)1142227501.
E-mail addresses: j.o.gil-posada@sheffield.ac.uk, jogp1234@yahoo.com (J.O. Gil Posada).

http://dx.doi.org/10.1016/j.jpowsour.2014.03.145

indicated by Eq. (1) (in this paper the forward reactions represent the charging process, likewise, the backward reactions represent the discharge process) [3,4].

$$Fe(OH)_2 + 2e^- \leftrightarrow Fe + 2OH^- \quad E^0 = -0.87\ V \tag{1}$$

Unfortunately, the charging efficiency of an iron electrode is drastically reduced by diverting part of the charging current in the wasteful evolution of hydrogen, as illustrated by Eq. (2).

$$2H_2O + 2e^- \leftrightarrow H_2 + 2OH^- \quad E^0 = -0.83\ V \tag{2}$$

Bismuth sulphide has been reported to decrease the hydrogen evolution reaction in NiFe cells by increasing the overpotential for hydrogen evolution [5,6]. During the process of charge and discharge, bismuth sulphide undergoes the following reaction:

$$Bi_2S_3 + 6e^- \leftrightarrow 2Bi + 3S^- \quad E^0 = -0.82\ V \tag{3a}$$

There are other elements with the capacity of reducing the evolution of hydrogen on NiFe cells, such as cadmium, lead and mercury; however, they are highly toxic and therefore, are not going to be considered in this investigation.

In this investigation, the performance of the NiFe cell was calculated based upon its columbic efficiency and utilization of electroactive material.

The charging efficiency was calculated by considering only two competing process (namely Eq. (1) and Eq. (2)) that take place during the charging of the iron electrode. So the following expression holds [5]:

$$\eta_Q = \frac{Q_{ch} - Q_H}{Q_{ch}} \times 100 \tag{3b}$$

Where η_Q is the coulombic efficiency, Q_{ch} is the total charge and Q_H is the charge wasted in hydrogen evolution.

The charge used for hydrogen evolution was calculated with the current of hydrogen evolution, which in turn was calculated by using the Tafel relationship [6–11].

3. Experimental

Iron electrodes were produced by coating strips of nickel foam (10 mm × 40 mm × 1.8 mm) with an iron active paste which consists of varying amounts of Fe, PTFE and Bi_2S_3. The chemicals and materials used to produce the electrodes were of the following specifications.

- Iron powder (purity 99.5%, <10 μm) from Alfa Aesar
- PTFE (Teflon 30-N, 59.95% solids) from Alfa Aesar
- Bismuth sulphide (purity 99.5%, <5.0 μm) from Sigma Aldrich

The procedure followed to produce our cells consists in the following steps:

i. Electrodes were made of Ni-foam by cutting strips of 4 cm × 1 cm
ii. Mixtures of Fe, PTFE and Bi_2S_3 were produced according to an experimental plan
iii. Every Ni-foam electrodes was coated with one of the mixtures prepared in ii
iv. Electrodes were vacuum dried for no less than 5 h
v. Repeat steps iii–iv until a constant amount of electro-active material was loaded onto the electrode
vi. Electrodes were vacuum dried for one day
vii. Cells were assembled and tested

In order to understand the composition effect of Fe, PTFE and Bi_2S_3 on cell performance, an experimental design was proposed to investigate the composition space described by Table 1.

By using the mixing rules in a three dimensional concentration space, a simplex centroid design based on a conventional central composite design was proposed.

Based upon Table 1 the experimental design was implemented to efficiently investigate the composition space and their incidence on the performance of NiFe cells. The final composition space is reported in Table 2.

Electro-active pastes, produced according to Table 2, were used to coat stripes of Ni foam. The electrodes thus produced, were then vacuum dried and the process repeated several times until the amount of electro-active material, iron in this case, was approximately 0.2 g.

Once produced, iron electrodes were tested in a three-electrode cell. Nickel electrodes (obtained from a commercial nickel–iron battery) where used as the positive electrode of the cell. The electrolyte was a concentrated solution of potassium hydroxide (28.5%). All potentials were measured against a mercury/mercury oxide (MMO) reference electrode ($E^0_{MMO} = +0.098$ V vs. NHE). Experiments of charge and discharge were performed on a 64 channel Arbin SCTS ±5 mA. An sketch of the cell test configuration can be found in Fig. 1.

4. Results and discussion

4.1. Charge and discharge

Experiments of charge and discharge were conducted at room temperature for at least 40 cycles. As shown in Fig. 2, cells were cycled from 0.6 to 1.4 V vs. MMO at a C/5 rate.

Typical charge and discharge voltage profiles for a NiFe cell can be found in Fig. 3.

Fig. 3 reveals there is a conditioning period where the cell undergoes internal re-structuration (this is until signal response reached the steady state), after that a stable pattern was achieved. Broadly speaking, this conditioning period was constantly achieved after 25–30 cycles.

The cells under consideration exhibit interesting performance characteristics after the conditioning period previously described. In fact, utilizations close to 23% and coulombic efficiencies near 33% are not uncommon. See Fig. 4.

Fig. 4 also reveals a capacity in the order of 250 mAh g^{-1}, which is a remarkable achievement, given the fact that we are using neither nano-size, nor ultrapure reactants.

From the experimental results obtained up to this point, we can conclude that there are good reasons to be confident that is possible to produce a NiFe cell with reasonable performance at a reasonable price.

4.2. Investigation of cell parameters

Table 2 lists the values of the coulombic efficiency calculated for our samples. As can be seen, the data exhibits large variability so a large number of replicates (9 in this case) were required to increase

Table 1
Experimental definition of factors and levels (concentrations in weight fraction).

Factor	Low	High
Bi_2S_3	0.5%	5%
PTFE	3%	12%
Fe	83%	96%

Table 2
Experimental design matrix (concentrations in weight fraction).

Cell	[Bi]	[PTFE]	[Fe]	η_Q
A	0.005	0.035	0.960	1.6 ± 0.5
B	0.025	0.040	0.935	16.2 ± 4.5
C	0.005	0.075	0.920	4.3 ± 0.5
D	0.005	0.075	0.920	4.8 ± 0.5
E	0.050	0.040	0.910	19.2 ± 6.5
F	0.025	0.080	0.895	28.4 ± 5.5
G	0.025	0.080	0.895	27.8 ± 5.5
H	0.005	0.115	0.880	2.8 ± 0.5
I	0.050	0.080	0.870	35.3 ± 8.5
J	0.050	0.080	0.870	34.8 ± 5.5
K	0.025	0.120	0.855	25.8 ± 9.5
L	0.050	0.120	0.830	33.7 ± 11.5

the force of the analysis. With this in mind, any sample whose coulombic efficiency lies more than two standard deviations from the mean was rejected.

In order to determine whether a relationship existed between the factors and responses (either coulombic efficiency or utilization of electroactive material) under investigation, the collected data was systematically analysed by using regression and multivariate analysis. In the present case, a second order Scheffé polynomial was used to model the response, according to Eq. (4).

$$\psi(\lambda_i, \chi_i) = \lambda_0 + \sum_{\xi=1}^{q} \lambda_\xi Y_\xi + \sum_{\xi=1}^{q-2} \sum_{\vartheta=\xi+1}^{q} \lambda_{\xi,\vartheta} Y_\xi Y_\vartheta \quad (4)$$

Where ψ represents the response, the λ's represent the expansion coefficients and Y's are the compositions. For a three component system, Eq. (4) can be used to express the response variable in terms of the compositions of any species used to produce the NiFe electrodes, in the following manner:

$$\eta_Q = \lambda_1 Y_F + \lambda_2 Y_B + \lambda_3 Y_P + \lambda_4 Y_F Y_B + \lambda_5 Y_F Y_P + \lambda_6 Y_B Y_P \quad (5)$$

Where η_Q represents the coulombic efficiency, the Y terms represent the weigh fraction of each component and the subscripts F, B and P correspond to iron, bismuth sulphide and PTFE respectively.

More often than not Scheffé polynomials are not capable to fully describe the intended response variables, especially when the values of the response variable span over several orders of magnitude. In such situations, surface response transformations can be used to improve the capability of such polynomials to mirror signal response(s).

In order to find the correct form of Eq. (5), electrodes were produced according to our experimental plan, in addition nine

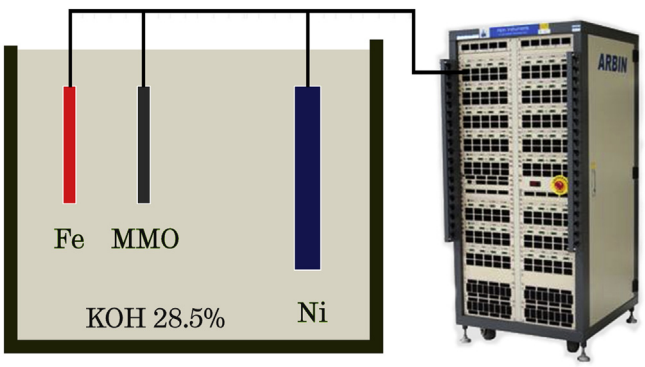

Fig. 1. Test cell configuration.

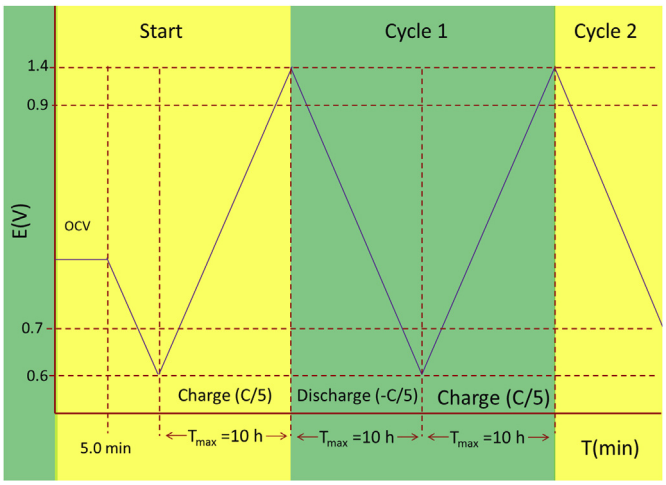

Fig. 2. Charge and discharge cell testing (vs. MMO).

replicates per electrode were used to minimise variability. From the experimental data, a quadratic regression model for the coulombic efficiency was obtained:

$$\eta_Q = -16721.69619Y_B - 3133.92384Y_P - 22.62635Y_F + 26045.27383Y_P Y_B + 17937.36661Y_F Y_P + 3674.08568Y_B Y_P \quad (6)$$

Where any positive sign in front of each composition term indicates a synergistic effect; likewise, any negative sign indicates an antagonistic effect.

The ANOVA test reveals an F value of 82.65, which implies that the overall model is significant; moreover, at the level of confidence $\alpha = 0.05$ all of the individual parameters of the model are significant.

It is always a good practise to check whether or not the fitted model provides an adequate approximation to the true system. In addition, it is always necessary to verify that none of the least

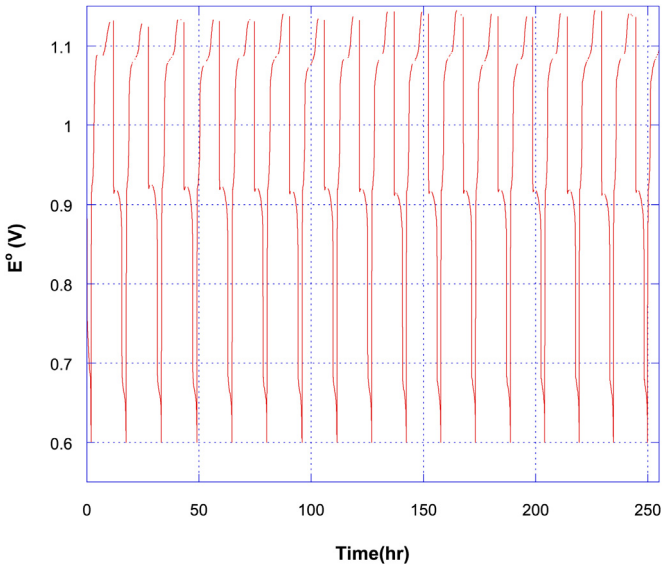

Fig. 3. Charge and discharge profile for a NiFe cell (sample J from Table 2) versus mercury/mercury oxide (MMO) reference electrode. Experimental cyclic conditions are shown in Fig. 2.

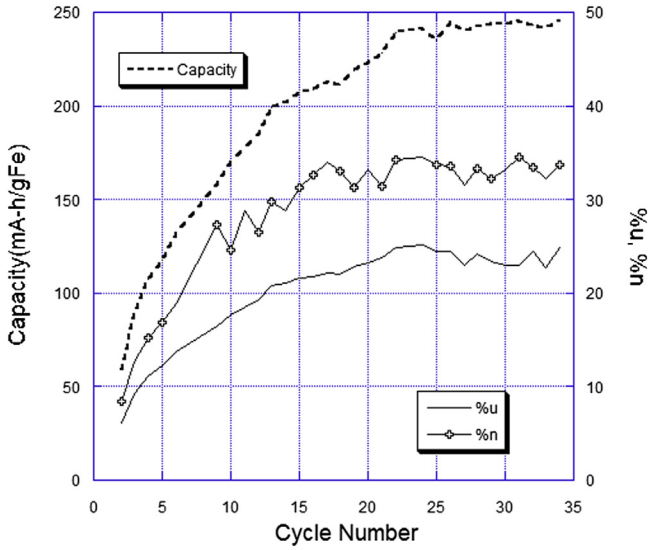

Fig. 4. Battery performance versus cycling number for a NiFe cell (sample J from Table 2).

squares regression assumptions are violated. In the present case, we had used not only graphical but also more rigorous tests for normality. Fig. 5 shows a graphic analysis for normality, in this case there is no evidence against normality.

The Shapiro–Wilk test, a non-parametric test for normality, also indicates there is no evidence against normality (p-value = 0.06678). This conclusion was corroborated by using the Kolmogorov–Smirnov test (p-value = 0.1997). We had found that at the level of confidence $\alpha = 0.05$, there is no evidence against normality.

By following the same line of thought, Eq. (5) can also be used to investigate the utilization of the electroactive material.

$$u_Q = -6238.250056Y_B - 695.130366Y_P - 6.600924Y_F + 10398.637920Y_PY_B + 6648.722580Y_FY_P + 827.632916Y_BY_P \quad (7)$$

The analysis of variance also reveals that second order Scheffé polynomials are well suited to investigate the electroactive material utilization problem. In this case, the F value is close to 276.8, which is large enough to consider the phenomenon is described by the model and not by chance. As with the coulombic efficiency, there is no evidence against normality (Shapiro–Wilk test reveals a p-value = 0.5482, likewise, the Kolmogorov–Smirnov test indicates a p-value = 0.3818, this is, both are significant). We conclude the Scheffé polynomials provide a means to investigate the composition space for the preparation of NiFe cells.

For the sake of completeness, we have compared our standard model (Eq. (5)) with selected models after standard transformations (such as logarithmic, radical, power, etc.). Second order Scheffé polynomials were used to analyse our transformed response variables (either coulombic efficiency or utilization of electroactive material). The second order Scheffé polynomial after a standard transformation takes the form:

$$\acute{\eta}_Q = \lambda_1 Y_B + \lambda_2 Y_P + \lambda_3 Y_F + \lambda_4 Y_P Y_B + \lambda_5 Y_F Y_B + \lambda_6 Y_F Y_P \quad (8)$$

Where the term $\acute{\eta}_Q$ represents the coulombic efficiency after any standard transformation. A similar expression can be written for the utilization of electroactive material.

Our experimental results indicate that the standard model (Eq. (5)) is well suited to analyse our signal responses; however, after a logarithmic transformation Eq. (8) renders a better fit. In fact, the residuals calculated by using Eq. (8) are lower than the residuals calculated by using Eq. (5). Eq. (8) finally takes the form:

$$\acute{\eta}_Q = \mathrm{Ln}(\eta_Q) = -1886.76121Y_B - 240.7539 - 1.51259Y_F + 2400.20208Y_PY_B + 2041.59978Y_FY_B + 289.25007Y_FY_P \quad (9)$$

We conclude that using the second order model after a logarithmic transformation is the correct way to investigate the coulombic efficiency in our NiFe cells.

Fig. 6 provides a three dimensional representation of Eq. 9

In the case of utilization of electroactive material, there is no need for a transformation. A residuals analysis reveals there are no meaningful differences when using Eq. (5) or Eq. (8) after some of

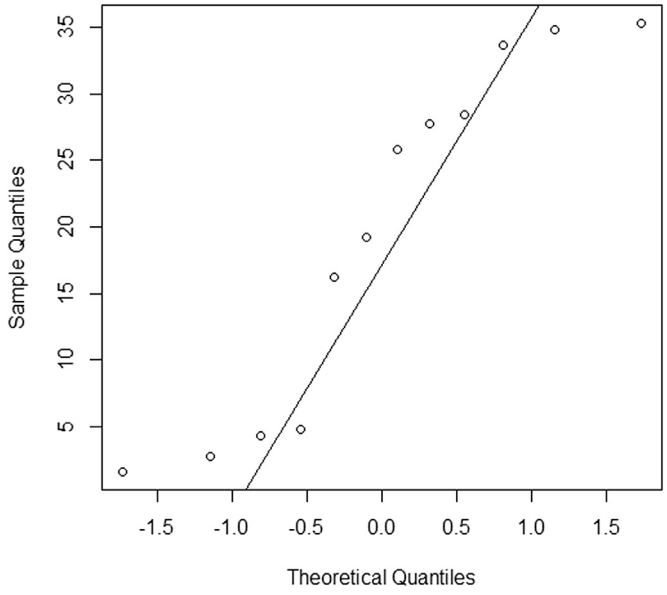

Fig. 5. Normal probability plot for coulombic efficiency residuals.

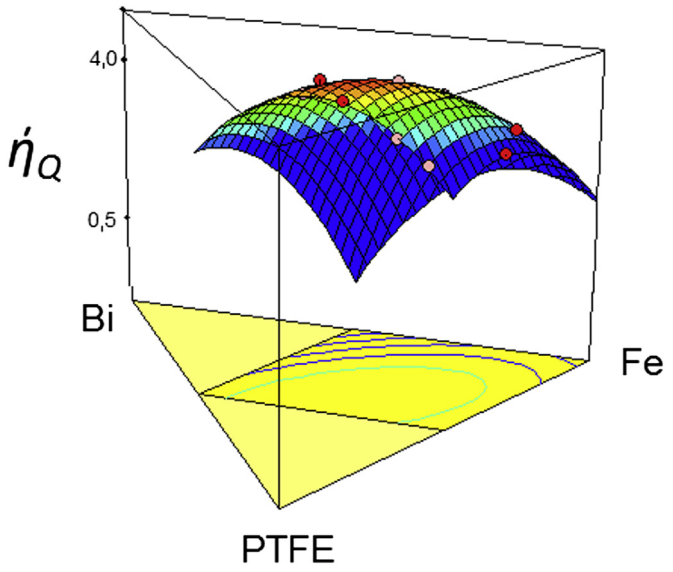

Fig. 6. Second order coulombic efficiency representation after a logarithmic transformation.

the most commonly used standard transformations (logarithmic, square and cubic roots).

We conclude that using the simplest second order model without any transformation is the correct way for investigating the utilization of electroactive material in our NiFe cells.

Fig. 7 provides a three dimensional representation of Eq. (7).

Table 3 shows that the predicted by the model coulombic efficiencies approximated the experimental ones. In general terms, the error was low (usually between 5 and 10%), Table 3 also reveals a larger error of 14.8% for sample A; however, this error is due to the small absolute value for the coulombic efficiency.

By looking at Table 3, it is clear that some samples (such as A, D or H) exhibit reasonably large deviations for the coulombic efficiency; however, the difference between the measured and the predicted by the model coulombic efficiencies never exceeds 2% units, so the second order model is well suited to investigate coulombic efficiency under our experimental conditions. Likewise, the second order model (without any transformation) exhibits a low variation, which is an indication of the correctness of the model.

Finally, a word of caution; although the second order model seems well suited to investigate our samples there is a very large variability between samples, and because of that, a large number of replicates per electrode is required.

4.3. Investigation of cell parameters

In order to find the optimal values that render the highest coulombic efficiency (and also the lowest evolution of hydrogen), we have used the fundamental theory of calculus to find stationary values of many-variable functions.

We are not going to give a presentation on how to find the maximum value of a differentiable function subject to a constraint (such as $\%Bi_2S_3 + \%PTFE + \%Fe = 100$). The details of such procedure can be found in most books of calculus. In order to facilitate the finding of conditions that maximise our objective function, we have produced a C/C++ program based on a simplex algorithm. Note that the process of minimization can be accomplished by using the same algorithm applied to the negative of the objective function.

The main problem to overcome in order to achieve a large scale utilization of NiFe cells, is to decrease the large evolution of hydrogen. Therefore, it was felt that our main objective was to optimize coulombic efficiency. Of course, we also require high utilization of electroactive material. By analysing the form of Eq. (6) (see Fig. 7), we had found that high values of utilization (26%–30%) are reached in the nearness of the region where coulombic efficiency is maximised.

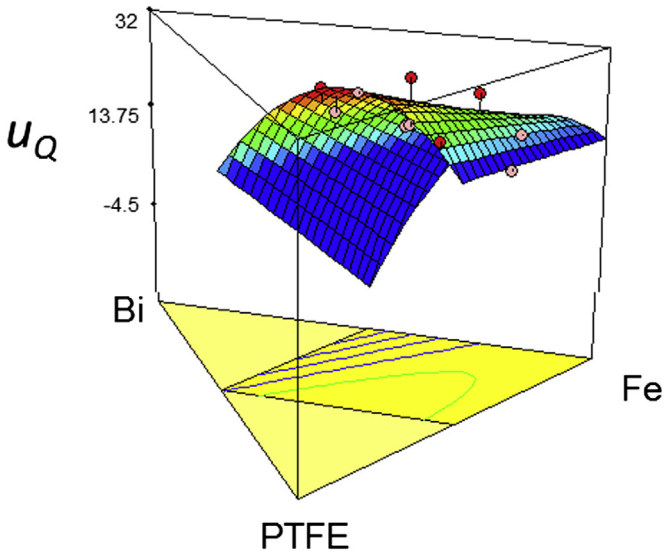

Fig. 7. Second order utilization of electroactive material surface response model.

Table 3
Coulombic efficiency and utilization of electroactive material for selected NiFe cells.

Cell	Experiment		Model		%Error	
	η_Q	u_Q	η_Q[a]	u_Q[b]	η_Q	u_Q
A	1.6	12.2	1.9	12.4	14.8	1.30
B	16.2	19.3	15.3	19.2	−5.6	−0.64
C	4.3	14.1	3.9	14.3	−8.7	1.68
D	4.8	14.6	3.9	14.3	−18.2	−1.80
E	19.2	19.8	17.8	19.7	−7.5	−0.36
F	28.4	23.5	30.2	23.2	6.4	−1.44
G	27.8	23.1	30.2	23.2	8.7	0.27
H	2.8	13.8	3.3	13.7	16.7	−0.96
I	35.3	27.2	37.6	26.6	6.6	−2.07
J	34.8	25.7	37.6	26.6	8.1	3.65
K	25.8	24.1	23.7	24.5	−8.4	1.66
L	33.7	31.2	31.6	30.9	−6.3	−0.97

[a] Logarithmic second order model.
[b] Second order model.

By taking into account the previous considerations, we have finally concluded, that battery performance is maximized at 3.98% Bi_2S_3 + 9.12%PTFE + 86.9%Fe (for the sake of simplicity we label this formulation with the letter *M*). In this case, coulombic efficiency was in the order of 48.6% and utilization of electroactive material close to 27.35%.

In order to corroborate the accuracy of the model, three more cells were produced at the optimal conditions already calculated (formulation *M*). After 40 cycles of charge and discharge, the coulombic efficiency for this sample was in the order of 44.51%, and the utilization of electroactive material close to 33.44%. In the case of the optimal cell, the deviation was larger than expected (−9.11% for the coulombic efficiency and 18.2% for the utilization of electroactive material), but still, the prediction made by the model is remarkable.

Due to the relatively large deviation at high coulombic efficiencies and utilization values, it is proposed to conduct more research in the nearness of the optimal sample (formulation *M*).

Fig. 8 shows coulombic efficiency and utilization of electroactive material for the NiFe cell prepared at the optimal conditions.

The optimization process has been successful in finding a set of concentrations where coulombic efficiency was maximised while keeping high utilization of electroactive material.

It has been reported that the capacity of the iron electrode is about 100–300 mAh g^{-1}. However, capacities up to 800 mAh g^{-1} has been achieved by nanostructuring the electrode [12–15]. In our case, we have achieved an incredible 325 mAh g^{-1} by using a relatively simple method and avoiding the use of ultra-pure reactants.

In order to further investigate the individual effect of metallic bismuth and sulphur in the columbic efficiency, the following formulations (based on formulation *M*) were compared:

- 3.98%Bi_2S_3 + 9.12%PTFE + 86.9%Fe
- 3.98%Bi_2S_3 + 9.12%PTFE + 85.9%Fe + 1%Bi
- 3.98%Bi_2S_3 + 9.12%PTFE + 84.9%Fe + 2%Bi
- 3.98%Bi_2S_3 + 9.12%PTFE + 85.9%Fe + 1%K_2S
- 3.98%Bi_2S_3 + 9.12%PTFE + 84.9%Fe + 2%K_2S

By using three replicates per formulation and at the level of confidence $\alpha = 0.05$, no meaningful differences between

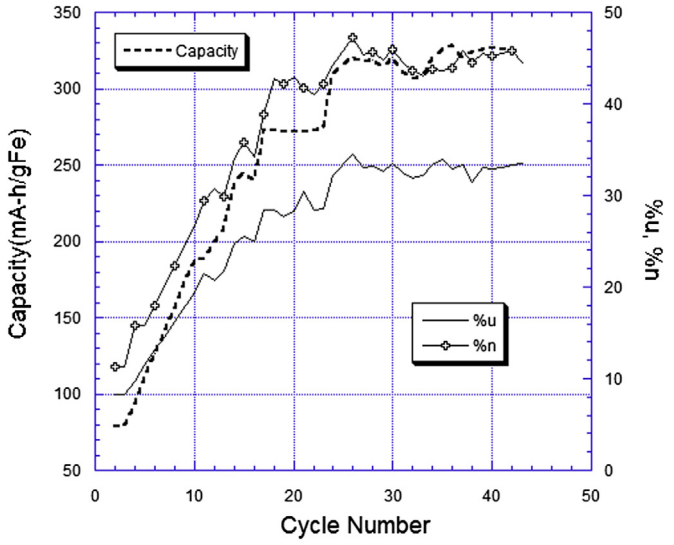

Fig. 8. Battery performance versus cycling number for cell *M* (3.98%Bi_2S_3 + 9.12% PTFE + 86.9%Fe).

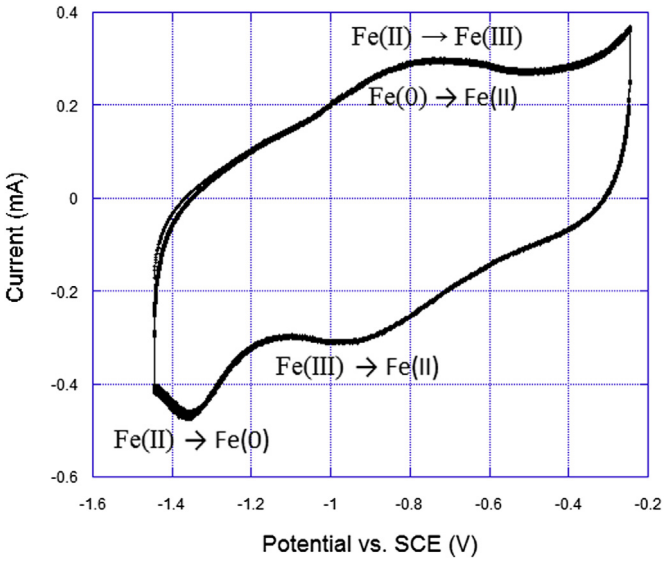

Fig. 9. Cyclic voltammetry of 3.98%Bi_2S_3 + 9.12%PTFE + 86.9%Fe in aqueous KOH 28.5% at a scan rate of 0.5 mV s^{-1}.

modifications of formulation *M* were found (results are not shown). In other words, neither metallic bismuth, nor soluble sulphide species coming from K_2S are responsible for the improvement in the performance of NiFe cells. This experimental observation indicates that metallic bismuth would not increase the coulombic efficiency of NiFe cells under strong alkaline conditions as has been suggested [5]. In addition, the use of potassium sulphide has proven that the presence of the soluble bisulfide anion (HS^-) does not increase much the coulombic efficiency of a NiFe cell.

As was explained, the charging efficiency of a NiFe cell is affected by the evolution of hydrogen (refer to Eq. (3)). It has been proposed that the evolution of hydrogen under alkaline conditions is determined by the passivation of the iron electrode. This process can be understood as the spontaneous formation of a surface oxide layer that prevents the iron electrode from corroding. Unfortunately, this process is poorly understood [16].

It has been reported that bismuth sulphide foments the passivation of the iron electrode [6]. Therefore, the functional groups of the form Fe—Bi—S or Fe—Bi, bismuth sulphide could be promoting the oxidation of the iron.

It has also been reported hydrogen can enter into transition metals such as iron during electrochemical process. In any aqueous cells, this process is promoted by reduced sulphur species such as HS^-, S^{2-} and H_2S [17–21]. In addition, it has been reported that hydrogen enhances the reduction of Fe(III) to Fe(II); any passive film on iron would consist on a structure that resembles a spinel (magnetite Fe_3O_4) or perhaps a defective maghemite (γ-Fe_2O_3), in general any other forms of iron would be possible [22].

It has been reported that hydrogen evolution and ingress into the iron electrode is strongly enhanced by renewal of the metal surface [23]. This observation confirms that the first few cycles of charge and discharge (conditioning period) are crucial for the final performance of the NiFe cell.

Finally, it is though that a synergistic effect between bismuth sulphide and the generation of surface area could explain the reactivity of the iron electrode.

4.4. Cyclic voltammetry

Cyclic voltammetry was used to investigate the electrochemical properties of the electroactive paste used to produce the NiFe cells (in 28.5% KOH). The electrode was investigated after conditioning (50 cycles of charge and discharge). Fig. 9 shows a typical cyclic voltammetry experiment of a NiFe cell.

The broad cathodic peak appearing in Fig. 9 at −0.8 V (vs. SCE) corresponds not only to the oxidation of Fe(II) to Fe(III) but also to the oxidation of Fe(0) to Fe(II), as given in the following (forward) equations:

$$Fe + 2OH^- \leftrightarrow Fe(OH)_2 + 2e^- \quad (10)$$

$$Fe(OH)_2 + OH^- \leftrightarrow FeO(OH) + H_2O + e^- \quad (11)$$

The cathodic peaks appear well differentiated at −0.9 V and −1.3 V (vs. SCE). The cathodic process are also given by Eq. (10) and Eq. (11) but in the backward sense. At even more cathodic potentials, the evolution of hydrogen by alkaline water decomposition was obtained. These results are in good agreement with recent publications [13,24].

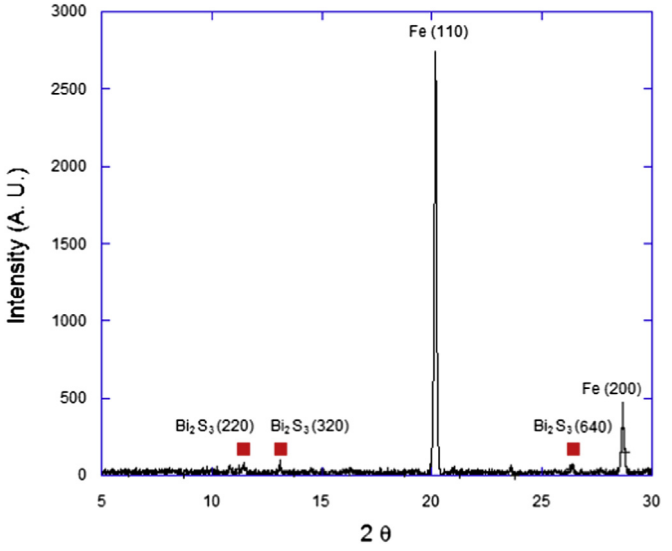

Fig. 10. XRD for 3.98%Bi_2S_3 + 9.12%PTFE + 86.9%Fe.

Our XRD results indicate the presence of α-Fe and $Fe(OH)_2$, but we have got no compelling evidence of all species partaking in Eq. (11). See Fig. 10.

It has been reported that metallic bismuth increases the overpotential for hydrogen evolution, thus reducing its production. During the charging of a NiFe cell, bismuth sulphide is transformed into elemental bismuth according to Eq. (3).

Fig. 10 suggests the formation of metallic bismuth in our cells is negligible. In general have we found no compelling evidence in favour or against metallic bismuth being responsible for any reduction in the evolution of hydrogen from NiFe cells.

5. Conclusions

The multivariate approach used in this work has been successful in facilitating the improvement of the performance of iron electrodes. The formulation developed after the optimization process (formulation *M*) has been found to show excellent performance, not only in terms of coulombic efficiency but in utilization of electroactive material; this formulation renders electrodes with large capacity close to 325 mAh g^{-1}.

Due to the relatively large deviation at high coulombic efficiencies and utilization values, it is proposed to conduct more research in the nearness of the optimal formulation.

Second order Scheffé polynomials are well suited to investigate the production of NiFe cells. In general terms, the model predicts reasonably well the properties of constructed cells; however, it is advisable to produce large numbers of cells to increase the statistical force of the analysis (decrease variability).

Our experimental results provide evidence suggesting that the theory that elemental bismuth prevents the evolution of hydrogen in NiFe cells under alkaline conditions is not entirely correct. In fact, under the experimental conditions, the addition of metallic bismuth did not reduce the evolution of hydrogen, nor it increased the coulombic efficiency. Therefore, it necessarily follows that there must be other species, probably in the surface of the electrode (such as sulphur containing molecules) acting in a synergistic way with metallic bismuth, so the evolution of hydrogen is reduced.

We believe that a synergistic effect between bismuth sulphide and the generation of surface area could explain the reactivity of the iron electrode.

The use of potassium sulphide has proven that the presence of the soluble bisulfide anion (HS^-) does not increase the coulombic efficiency of a NiFe cell.

Cyclic voltammetry has confirmed two redox process occurring during the charge and discharge of a NiFe cell, they are the conversion of Fe(II) to F(III) and the conversion of Fe(0) to Fe(II).

Acknowledgements

The authors would like to acknowledge the U.K. Engineering and Physical Sciences Research Council for supporting this work (EP/K000292/1; SPECIFIC Tranche 1: Buildings as Power Stations). Finally, the authors would like to thank Dr. Anthony J. R. Rennie from Chemical and Biological Engineering, University of Sheffield.

References

[1] C.-Y. Kao, Y.-R. Tsai, K.-S. Chou, J. Power Sources 196 (2011) 5746–5750.
[2] A. Chaurey, S. Deambi, Renew. Energ. 2 (1992) 227–235.
[3] G. Halpert, J. Power Sources 12 (1984) 177–192.
[4] A.K. Shukla, S. Venugopalan, B. Hariprakash, J. Power Sources 100 (2001) 125–148.
[5] A.K. Manohar, S. Malkhandi, B. Yang, C. Yang, G.K.S. Prakash, S.R. Narayanan, J. Electrochem. Soc. 159 (2012) A1209–A1214.
[6] T.S. Balasubramanian, A.K. Shukla, J. Power Sources 41 (1993) 99–105.
[7] E. Gileadi, E. Kirowa-Eisner, Corros. Sci. 47 (2005) 3068–3085.
[8] E. McCafferty, Corros. Sci. 47 (2005) 3202–3215.
[9] I.A. Ammar, S. Darwish, Electrochim. Acta 12 (1967) 833–841.
[10] M.D. Arce, H.L. Bonazza, J.L. Fernández, Electrochim. Acta 107 (2013) 248–260.
[11] R. Notoya, Electrochim. Acta 42 (1997) 899–905.
[12] P. Periasamy, B. Ramesh Babu, S. Venkatakrishna-Iyer, J. Power Sources 12 (1996) 9–14.
[13] H. Wang, Y. Liang, M. Gong, Y. Li, W. Chang, T. Mefford, J. Zhou, J. Wang, T. Regier, F. Wei, H. Dai, Nat. Commun. 3 (2012) 1–8.
[14] Z. Liu, S.W. Tay, X. Li, Chem. Commun. 47 (2011) 12473–12475.
[15] M.K. Ravikumar, T.S. Balasubramanian, A.K. Shukla, J. Power Sources 56 (1995) 209–212.
[16] I. Diez-Perez, F. Sanz, P. Gorostiza, Electrochem. Commun. 8 (2006) 1595–1602.
[17] G. Williams, H.N. McMurray, R.C. Newman, Electrochem. Commun. 27 (2013) 144–147.
[18] I. Flis-Kabulska, J. Flis, T. Zakroczymski, Electrochim Acta 52 (2007) 7158–7165.
[19] A. Barnoush, H. Vehoff, Acta Mater. 58 (2010) 5274–5285.
[20] C.L. Yu, T.P. Perng, Acta Metall. Mater. 36 (1991) 1091–1099.
[21] J. Flis, S. Ashok, N.S. Stoloff, D.J. Duquette, Acta Metall. Mater. 35 (1) (1987) 2071–2079.
[22] H.B. Shao, J.M. Wang, W.C. He, J.Q. Zhang, C.N. Cao, Electrochem. Commun. 7 (2005) 1429–1433.
[23] I. Flis-Kabulska, Electrochem. Commun. 11 (2009) 54–56.
[24] R. Solmaz, G. Karda, Electrochim. Acta 54 (2009) 3726–3734.